Proc. Natl. Acad. Sci. USA
Vol. 74, No. 7, pp. 2607–2611, July 1977
Chemistry

Excited state lifetimes in cytochromes measured from Raman scattering data: Evidence for iron–porphyrin interactions

(metalloproteins/heme proteins/optical properties)

J. M. FRIEDMAN†, D. L. ROUSSEAU†, AND F. ADAR‡

† Bell Laboratories, Murray Hill, New Jersey 07974; and ‡ Department of Biochemistry and Biophysics, University of Pennsylvania, Philadelphia, Pennsylvania 19104

Communicated by R. G. Shulman, April 11, 1977

ABSTRACT **Resonance Raman scattering excitation profile data have been obtained on ferrocytochromes *c* and b_5 in the α absorption band region. We observe in cytochrome *c* that the shape of the excitation profile agrees with the absorption band shape, while in cytochrome b_5 it does not. In addition, we observe in cytochrome b_5 a linewidth substantially larger than that in cytochrome *c*. From our data we conclude that the excited state lifetime in cytochrome *c* is longer than that in cytochrome b_5 and that in cytochrome b_5 the relaxation of the π–π^* excited state configuration of the porphyrin ring is different in the *x* direction than in the *y* direction. Possible origins of these effects due to coupling to the *d*–*d* transitions of the iron atom are discussed.**

The molecular and electronic properties of heme proteins have been heavily studied by a wide variety of techniques in an effort to understand on a molecular level the mechanisms of the oxidation–reduction processes. Most electronic structure information about the porphyrin macrocycle of these proteins has been obtained from the analysis of absorption (1) and fluorescence (2) data, but more recently several groups (refs. 3–10 and references cited in ref. 8) have applied the technique of resonance Raman scattering to these systems to determine molecular symmetry and electronic structure properties. In this study we have examined the well-known splitting of the α-absorption band in heme proteins by obtaining resonance Raman excitation profile data, i.e., the intensity of the Raman scattering as the excitation frequency is tuned through the absorption band. The α-bands of both ferrocytochrome *c* and ferrocytochrome b_5 were investigated. Our data demonstrate that the excited state lifetime resulting from the $Q_{0,0}$ transition (α-band) is shorter in cytochrome b_5 than it is in cytochrome *c*. They also show that in cytochrome b_5 the excited state lifetimes of the split α-band differ substantially. Such a lifetime difference is absent in cytochrome *c*. We discuss possible explanations for these differences in terms of nonradiative relaxation via *d*–*d* transitions.

METHODS AND MATERIALS

Cytochrome b_5 was prepared from calves liver by the method of Omura and Takesue (11). It consists of protoporphyrin IX iron(II) in which the iron atom is bound to the protein through histidine ligands (12). Cytochrome *c* was purchased commercially (Sigma type VI). The iron atom of the heme *c* is attached to the protein by histidine and methionine residues and the porphyrin ring is also attached to the protein by two thio-ether linkages to cysteine residues (13). Both cytochromes were reduced with sodium dithionite at pH 7. Samples in aqueous solution were placed on the cold finger of a Heli-Tran Dewar flask (Air Products) and cooled to about 6 K for the low-temperature experiments. Raman spectra were obtained with standard instrumentation utilizing dye laser sources to obtain tunability in the excitation frequency over the range of the α-band. To obtain the excitation profiles the intensities of the hemeprotein, Raman lines were compared to the intensity of either the ice Raman lines or the strong Raman line at 981 cm^{-1} of SO_4^{2-} [$(NH_4)_2SO_4$] that was added as a Raman intensity reference. Low-temperature absorption spectra were obtained by looking at the spectrum of white light scattered from the frozen sample and comparing it with the light scattered from a diffuse scatterer as well as by conventional transmission techniques using a Cary 15 spectrometer.

Abbreviation: fwhh, full width at half height.

RESULTS

Electronic Absorption Spectra of Cytochromes. The absorption spectra of hemeproteins and porphyrins have been extensively studied for many years and the assignment of the strong bands in the visible region is now well established (1). The strong features in this region result from two π–π^* transitions of the porphyrin ring. The strongest band in the range of 3900–4500 Å results from the addition of the electronic moments of the two transitions and is termed the Soret band. The weaker band in the 5400–6000 Å region results from the difference of the two nearly equal electronic moments. It is termed the α-band ($Q_{0,0}$ transition). To the blue of the α-band (below 5400 Å) there lies a vibronic sideband that is referred to as the β band ($Q_{0,1}$ transitions).

The absorption spectra of reduced cytochrome *c* and cytochrome b_5 obtained at about 6 K are presented in Fig. 1. We focus our attention on the α-bands, which for cytochrome *c* and cytochrome b_5 are centered at about 5450 Å and about 5550 Å, respectively. In both instances the α-band is split. This splitting is characteristic of many low-spin ferrohemeproteins and results from the removal of the double degeneracy of the lowest excited state of the porphyrin ring, probably due to the influence of the protein environment (14). Indeed, in the recent investigation (14) of a series of low-spin FE^{2+} model heme complexes no splittings or asymmetries of the $Q_{0,0}$ transition could be observed. These differences between the model compounds and the proteins presumably result from a preferred orientation of the imidazole rings of the histidine residues with respect to the heme plane, resulting from the protein structure (14).

As may be seen from Fig. 1, the splitting in cytochrome *c* is about 100 cm^{-1}, with both peaks having roughly the same widths. In cytochrome *c* the lower-frequency component is more intense than the higher-frequency component. In cytochrome b_5 the splitting of the α-band is larger (about 200 cm^{-1}). The two components do not have the same line shape in cytochrome b_5, but instead the lower-frequency peak is broader than the one at higher frequency.

Resonance Raman Scattering from Cytochromes. The

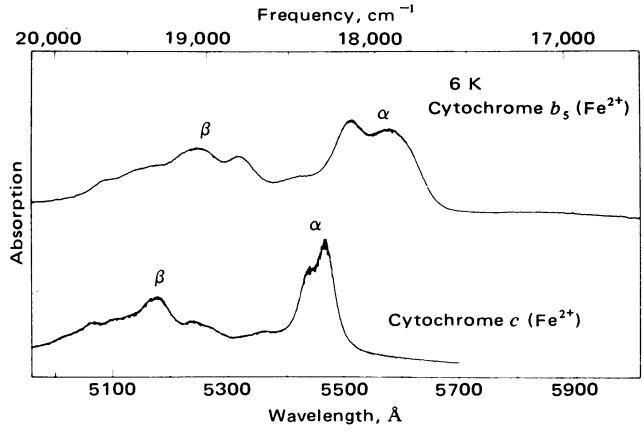

FIG. 1. Absorption spectra of ferrocytochrome c and b_5 in the region of the $Q_{0,0}$ (α-band) and $Q_{0,1}$ (β-band) transitions obtained on low-temperature samples (about 6 K).

low-temperature Raman spectra obtained with excitations in the region of the α-band of cytochrome c are shown in Fig. 2. Similar quality spectra were obtained from cytochrome b_5. Depicted in this figure are representative spectra originating from excitation slightly to the red and to the blue of the α-band as well as directly on resonance. The observed frequencies and behavior of the modes correspond to those of earlier work done at room temperature (3–5, 15, 16), although at low temperature with the improved signal-to-noise ratio we do observe many low-frequency modes that were not seen in the high-temperature studies.

As in room-temperature studies (7, 17, 18), relaxed fluorescence can also be seen in our spectra. See spectrum E especially. In this work we note that the Raman scattering remains on a nearly flat background as the excitation is tuned from the low energy side of the α-band to the blue of the first peak in the α-band. As the excitation then becomes resonant with the higher-energy peak a weak fixed-frequency background starts to emerge beneath the Raman scattering. Once the excitation is to the blue of the α-band the broad background progressively becomes a greater fraction of the re-emission yield, and remains at fixed absolute energy, while the Raman scattering shifts with the excitation frequency.

As compared to room-temperature solution data, the low-temperature data have increased signal-to-noise ratios due to reduction of thermal population effects. The qualitative features and mode frequencies remain the same. This is an expected result in that the resonance Raman scattering experiment is only probing the properties of the porphyrin ring due to the strong enhancement of the porphyrin ring modes resulting from the π–π^* electronic transitions. No vibrational modes due to the proteins are observed. Changing the external environment of the protein by freezing may therefore exert an influence of the protein periphery but it does not significantly influence the chromophore, which is isolated in a protein cage. Due to this isolation effect, conclusions about the porphyrin in the biologically active phases may be drawn from the results of low-temperature experiments in which the quality of the spectra is sufficient to obtain quantitative information.

For both cytochrome c and cytochrome b_5 we have obtained resonance Raman scattering excitation profiles over the region of the α-band. Such data are particularly useful for determining the origin of line-broadening mechanisms as well as giving excited state *lifetime* information (19). This information is only readily extractable in the limit where the contributing excited state levels are widely separated in energy and where the

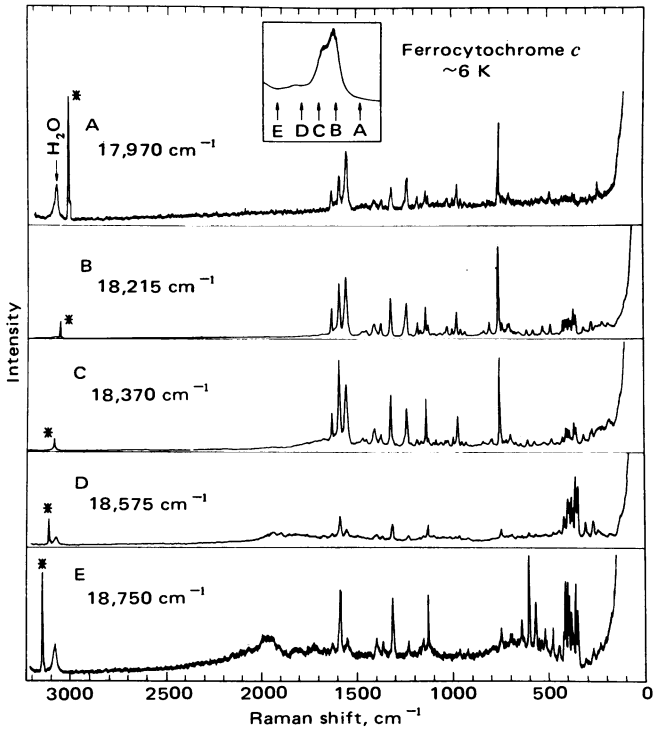

FIG. 2. Raman spectra of ferrocytochrome c obtained at about 6 K. Spectra obtained with representative excitation frequencies (A–E) throughout the α-band absorption region are presented. The excitation frequencies are listed on the left and indicated by the arrows on the absorption spectrum in the *inset*. The band in each spectrum marked by an asterisk is a grating ghost. The sensitivity and the laser power for each spectrum differ, but the relative intensities of the Raman lines between spectra may be assessed by comparison with the constant intensity ice line near 3080 cm^{-1}.

Raman cross section derives nearly all its intensity from a single resonant state. Such is the case for the cytochromes, but for a case where this does not hold see ref. 20. The data in the present work were obtained by measuring the intensity of a Raman emission line as a function of the incident laser frequency. For both cytochromes maxima were observed in the region of the α-band as well as in the region of the β-band. The latter maxima

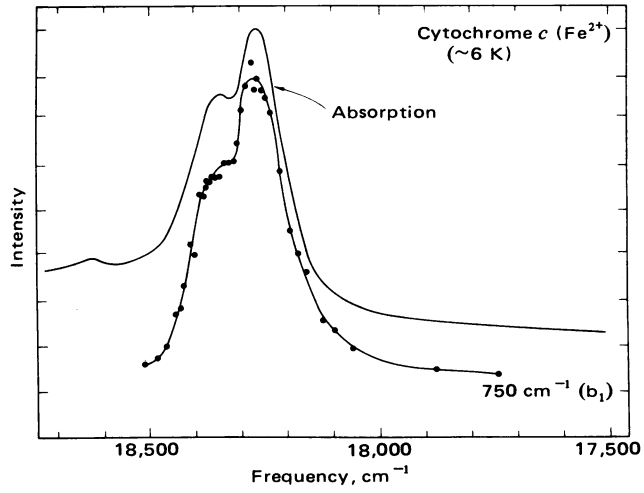

FIG. 3. Resonance Raman excitation profile of the 750 cm^{-1} mode of ferrocytochrome c in the region of the α-band. The upper solid line is the absorption spectrum and the points are the experimental Raman intensity data. The line drawn through the points is to guide the eye.

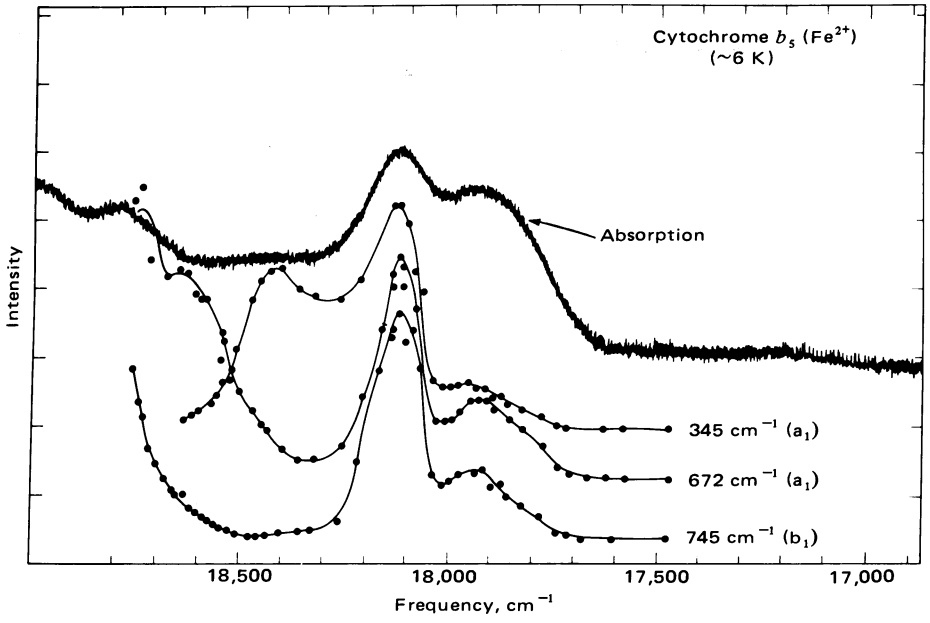

FIG. 4. Resonance Raman excitation profiles of several modes of ferrocytochrome b_5 in the region of the α-band. The upper trace is the absorption spectrum. The points are the experimental data and the lines drawn through them are to guide the eye.

were shifted from the α-band maxima by the spacing of the vibrational mode being studied. With the exception of the very-low-frequency modes where there is considerable uncertainty due to the Rayleigh wing background, the modes of a given symmetry species behaved the same for a given material.

In Fig. 3 we present the excitation profile of the 750 cm^{-1} b_1 mode (assuming a C_{4v} symmetry for the porphyrin ring) of cytochrome *c*, which is typical of the high-energy modes of this protein. This excitation profile exhibits roughly the same splitting in the α-band (about 100 cm^{-1}) as is observed in the absorption. The relative intensities of the two peaks are also approximately the same in the excitation profile as in the absorption shape, but on the high-energy side of the α-band the excitation profile drops to about the same level as on the low-energy side, thereby completely resolving the $Q_{0,0}$ transition in contrast to the behavior of the absorption. The widths of the two split components of the α-band appear to be the same in the excitation profile and in the absorption. [We estimate a full width at half height (fwhh) of about 120 cm^{-1}.]

In Fig. 4 we present typical excitation profiles for the cytochrome b_5 modes. In marked contrast to the cytochrome *c* data, the relative intensities of the two peaks for the α-band seen in the excitation profiles grossly deviate from the intensity pattern observed in the absorption spectra. It can be seen in Fig. 4 that in the excitation profile the ratio of the peak intensity of the broader low-frequency peak to that of the high-frequency peak is much smaller than the ratio observed in the absorption spectrum. This observation holds for all the Raman peaks that show intensity enhancement for excitation in the α-band. The splitting of the two peaks is the same as that observed in the absorption spectrum (about 200 cm^{-1}), and we estimate the fwhh linewidth of the low-energy peak to be about 240 cm^{-1} and the high-energy peak to be about 140 cm^{-1}.

DISCUSSION

The Raman spectra for both α-band peaks in both of the cytochromes show uniform enhancement of the fundamentals of nontotally symmetric modes with no enhancement of the corresponding overtones and combinations. This behavior is exactly what is expected (7) for resonances with vibronic origins in porphyrin rings and eliminates the possibility that the splitting results from a 0,0 and 0,1 transition or a 0,0 plus a phonon wing. Our data confirm that both peaks in the α-bands of both cytochromes originate from 0,0 transitions and the splitting is therefore indicative of a nuclear configuration of the porphyrin π^* electrons in which the *x* and *y* directions are inequivalent.

Monochromatic excitation in or near the broad α-band absorptions results in sharp re-emission. This may result from either a Raman scattering process due to interaction with a broad homogeneous absorption band or a fluorescence process from distinct chromophoric sites (an inhomogeneous distribution) each with its characteristic absorption and fluorescence (Personov effect) (21, 22). The importance of the latter effect in our data is minimal. For excitation to the blue of the α-band a broad diffuse band is observed in addition to the sharp discrete lines. In the emission spectrum this broad band is observed at the same frequency as the α-band in the absorption spectrum and it does not shift with excitation wavelength. We attribute it to relaxed fluorescence.[§] Because it has roughly the same width as the absorption line, this indicates that the full width of the α-band is due to homogeneous broadening. If the band were primarily inhomogeneously broadened, the relaxed fluorescence would also be sharp. Furthermore, the low quantum yield for re-emission (17, 18) indicates a very short nonradiative lifetime, which is consistent with a large homogeneous broadening and inconsistent with an inhomogeneous distribution of sharp absorption lines.

Analysis of excitation profile data of high-frequency vibrational modes over a homogeneously broadened line will give excited state lifetimes directly because the profile is free of

[§] Our recent experiments have demonstrated that β-band excitations generate both Raman emission and an excitation frequency-independent relaxed emission from the zero vibrational level of Q. Excitation to the blue of the β-band generates, in addition to Raman emission, relaxed emission as above, and a partially relaxed emission from excited vibrational levels of the Q electronic state.

low-lying $Q_{0,1}$ transitions present in the blue edge of an absorption line. From the representative excitation profile of the cytochrome *c* 750 cm^{-1} fundamental mode the width of both $Q_{0,0}$ peaks is about 120 cm^{-1} (fwhh), corresponding to a lifetime of about 45 fsec (45×10^{-15} sec) for both the *x* and *y* members of the α-band. From the corresponding excitation profile of cytochrome b_5 (745 cm^{-1} mode) we obtain a width of 240 cm^{-1} for the low-energy component and a width of 140 cm^{-1} for the high-energy component. These correspond to lifetimes of about 20 fsec and about 40 fsec, respectively. The difference in the lifetime of the two members of a nearly degenerate level is quite surprising and is in fact related to another unusual observation: in the excitation profiles for cytochrome *c* the two α-band peaks have the same intensity relation as observed in the absorption. In contrast, in cytochrome b_5 the intensity relationship is clearly different. To understand the implications of this observation it is necessary to consider the origin of the Raman scattering intensity and its relationship to the absorption.

The absorption cross section, *A*, for an isolated resonant adiabatic state, *i*, may be described (23) by the following proportionality:

$$A_{g\to i} \propto \frac{|V_{gi}|^2\Gamma_i/2}{(E_i - E)^2 + \left(\frac{\Gamma_i}{2}\right)^2}. \qquad [1]$$

Here V_{gi} is the matrix element for radiative coupling between the ground state *g* and the excited state *i*. Γ_i is the homogeneous width of the excited state of energy E_i and *E* is the incident photon energy. The width Γ_i consists of a sum of the widths due to radiative Γ_i^R and nonradiative Γ_i^{NR} decay channels.

For resonance Raman scattering from the initial state *g* to the final state *f* via the intermediate state *i* we may write (23) the intensity, *R*, as

$$R_{gf} \propto \frac{|V_{gi}|^2(\Gamma^R_{i\to f})/2}{(E_i - E)^2 + \left(\frac{\Gamma_i}{2}\right)^2} = \frac{A_{gi}\Gamma^R_{i\to f}}{\Gamma_i}. \qquad [2]$$

In this expression $\Gamma^R_{i\to f}$ is the contribution to the total width Γ_i due to the radiative coupling of the intermediate state *i* to the final state *f*.

In the cytochromes the nonradiative processes are much faster than the radiative decay (17, 18), so that Γ_i^{NR} is roughly 10^4 times larger than Γ_i^R. Thus, $\Gamma_i \simeq \Gamma_i^{NR}$. The differences in the excitation profiles in the two cytochrome compounds studied here therefore become clear. In cytochrome *c* both components of the *x,y*-split α-band have the same lifetime, so the Raman scattering intensity R_{gf} has the same frequency dependence as does the absorption. On the other hand, in cytochrome b_5 one component of the *x,y* doublet relaxes faster through the nonradiative decay channels than the other does. Therefore we see from the right-hand side of the equality in Eq. 2 that because $\Gamma_i \simeq \Gamma_i^{NR}$ the intensities of the two components do not behave the same in Raman scattering as they do in absorption, the nonradiative decays of the two components differ. This of course follows from the fact that at exact resonance ($E_i = E$) the absorption cross section varies as $1/\Gamma_i$ and the Raman intensity varies as $1/\Gamma_i^2$. We conclude from both the widths we observe in the excitation profile and from the relative intensities of the two components, that the lifetime of the lower-energy *x,y*-split component of the doublet has a shorter nonradiative relaxation time than its high-energy partner.

It has been pointed out in the past that the rather large widths of the absorption bands of the heme proteins result from nonradiative coupling of the π-π^* states to excited states involving the *d* orbitals of the iron atom (24). In the ferrocytochromes, the *x,y*-polarized *d*-*d* transitions are expected to couple most strongly to the π-π^* transitions. We may conclude from our data that the coupling of $Q_{0,0}$ transitions to the *d*-*d* transitions in cytochrome b_5 is stronger than it is cytochrome *c*. In addition it is clear that the *x,y* symmetry of the nonradiative decay has broken down in cytochrome b_5. An unequivocal explanation of the origin of the observed differences in relaxation rates awaits a careful measurement of the *d*-*d* transition energies through a circular dichroism experiment (25, 26). Some tentative conclusion and possibilities may be discussed, however.

In both cytochromes the splitting of the α-band results from a rhombic distortion of the porphyrin macrocycle. Due to this distortion the matrix elements coupling the porphyrin orbitals to the iron orbitals in cytochrome b_5 may be different in the *x* and *y* directions, resulting in the different relaxation rates of the *x* and *y* components that we observe. In addition, the field about the iron atom may be distorted such that, for example, the $d_{xz} \to d_{z^2}$ and the $d_{yz} \to d_{z^2}$ transitions differ in energy. The differences in the nonradiative lifetimes between the *x* and *y* components of the α-band in cytochrome b_5 could then result from inequivalent decay paths available to each of the components. Alternatively, the difference in the nonradiative decay times of the *x* and *y* components of cytochrome b_5 may be due to the presence of a *d*-*d* transition or charge transfer transition in near coincidence with one of the *x,y*-split components (the low-energy one) of the α-band. As a result, that component may decay more rapidly than the other one, accounting for the lifetime differences. Circular dichroism measurements in the near infrared region should be very useful in helping to sort out these possibilities.

Our data also demonstrate a clear difference in the nonradiative decay times of cytochrome *c* and cytochrome b_5. If we assume these homologous systems obey the energy gap law (27) for radiationless transitions, then we expect on the basis of comparative lifetimes that the in-plane *d*-*d* transitions in cytochrome b_5 will be closer in energy to the $Q_{0,0}$ transition than they are in cytochrome *c*. Again circular dichroism measurements on cytochrome b_5 would be useful. If the hemeproteins form a homologous group, then it might be possible to predict the relative energies of the *d*-*d* transitions with respect to the π-π^* transitions from an analysis of Raman data such as that presented here. This information is extremely important because the degree of interaction between the porphyrin π electrons and the iron *d* orbital electrons may influence the hemeprotein redox potentials and the dynamics of the pathway for electron transport, as well as other biologically relevant parameters.

The costs of publication of this article were defrayed in part by the payment of page charges from funds made available to support the research which is the subject of the article. This article must therefore be hereby marked "advertisement" in accordance with 18 U. S. C. §1734 solely to indicate this fact.

1. Gouterman, M. (1961) *J. Mol. Spectrosc.* **6**, 138–163.
2. Seybold, P. G. & Gouterman, M. (1969) *J. Mol. Spectrosc.* **31**, 1–13.
3. Spiro, T. G. & Strekas, T. C. (1972) *Proc. Natl. Acad. Sci. USA* **69**, 2622–2626.
4. Nafie, L. A., Pezolet, M. & Peticolas, W. L. (1973) *Chem. Phys. Lett.* **20**, 563–568.
5. Friedman, J. M. & Hochstrasser, R. M. (1973) *Chem. Phys.* **1**, 457–467.

6. Adar, F. & Erecinska, M. (1974) *Arch. Biochem. Biophys.* **165,** 570–580.
7. Friedman, J. M. & Hochstrasser, R. M. (1976) *J. Am. Chem. Soc.* **98,** 4043–4048.
8. Sunder, S. S., Mendelsohn, R. & Bernstein, H. J. (1975) *J. Chem. Phys.* **63,** 573–580.
9. Collins, D. W., Champion, P. M. & Fitchen, D. B. (1976) *Chem. Phys. Lett.* **40,** 416–419.
10. Shelnutt, J. A., Yu, W. T., Chang, R. C. C., Cheung, L. D. & Felton, R. H. (1976) in *Proceedings of Fifth International Conference on Raman Spectroscopy,* eds. Schmid, E., Braudmuller, J., Kiefer, W., Schrader, B. & Schratter, H. (H. F. Schulz, Publ., Freiburg), p. 336.
11. Omura, T. & Takesue, S. (1970) *J. Biochem. (Tokyo)* **67,** 249–257.
12. Mathews, F. S., Levine, M. & Argos, P. (1972) *J. Mol. Biol.* **64,** 449–464.
13. Kakudo, M. (1975) *Adv. Biophys.* **7,** 163–191.
14. Wagner, G. C. & Kassner, R. J. (1975) *Biochem. Biophys. Res. Commun.* **63,** 385–391.
15. Adar, F. (1975) *Arch. Biochem. Biophys.* **170,** 644–650.
16. Friedman, J. & Hochstrasser, R. M. (1975) *Chem. Phys. Lett.* **32,** 414.
17. Friedman, J. M. & Hochstrasser, R. M. (1974) *Chem. Phys.* **6,** 155.
18. Adar, F., Gouterman, M. & Armowitz, S. (1976) *J. Phys. Chem.* **80,** 2184–2190.
19. Penner, A. P. & Siebrand, W. (1976) *Chem. Phys. Lett.* **39,** 11–13.
20. Friedman, J. M., Rousseau, D. L. & Bondybey, V. E. (1976) *Phys. Rev. Lett.* **37,** 1610–1613.
21. Personov, R. K., Al'Shits, E. I. & Bykovskaya, L. A. (1972) *Opt. Commun.* **6,** 169–173.
22. Marchetti, A. P., McColgin, W. C. & Eberly, J. H. (1975) *Phys. Rev. Lett.* **35,** 387–390.
23. Nitzan, A. & Jortner, J. (1972) *J. Chem. Phys.* **57,** 2870–2889.
24. Hochstrasser, R. M. (1971) in *Probes of Structure and Function of Macromolecules and Membranes,* eds. Chance, B., Lee, C. & Blaise, J. K. (Academic Press, New York), Vol 1, p. 57.
25. Eaton, W. A. & Charney, E. (1969) *J. Chem. Phys.* **51,** 4502–4505.
26. Sutherland, J. C. & Klein, M. P. (1972) *J. Chem. Phys.* **57,** 76–86.
27. Jortner, J., Rice, S. A. & Hochstrasser, R. M. (1969) in *Advances in Photochemistry,* eds. Noyes, W. A., Pitts, J. N. & Hammond, G. (Wiley, New York), Vol. 7, pp. 149–309.